Progress In Electromagnetics Research C, Vol. 80, 221–231, 2018

A Broad-Side Coupled SRR Inspired CPW Fed Dual Band Antenna for WiMAX and WAVE Applications

Nambiyappan Thamil Selvi[1, *], Palavesa Thiruvalar Selvan[2], Shanmugaih P. K. Babu[3], Ramasamy Pandeeswari[4], and Raphael Samson Daniel[4]

Abstract—In present scenario, this paper intends to demonstrate the practicality of a miniaturized coplanar waveguide fed metamaterial inspired antenna that can be effectively operated at dual bands. A broad-side coupled Split Ring Resonator is used to obtain dual bands with an impedance bandwidth (−10 dB) of 840 MHz (3.00–3.84 GHz) and 310 MHz (5.94–6.25 GHz), which resonates at dual bands, viz., 3.42 GHz and 6.07 GHz. The impedance bandwidth ($S_{11} < -10$ dB) is 25% for the first band and 5.1% for the second band. The size of the antenna is $31 \times 25 \times 1.6$ mm^3 realized on a low-cost FR-4 Epoxy substrate. This antenna can be effectively utilized in worldwide interoperability for microwave access (WiMAX) and wireless access in vehicular environments (WAVE) applications. The prototype of the proposed antenna is fabricated and measured. Simulated and measured results are in agreeing nature. Experimental and simulated analyses of the antenna including parametric and dispersion characteristics are dealt in this communication.

1. INTRODUCTION

An exponential growth in the field of communication has created a mandate for multi-band antennas for various wireless communication applications in a single system. Electromagnetic metamaterials are homogeneous artificially engineered structures derived from sub-wavelength configuration instead of composite materials [1]. Owing to unusual property, they exhibit negative refractive index, reverse of Snell's law and Doppler effect. These materials are either single negative with alternatives ε-negative [ENG] and μ-negative [MNG], or double negative [DNG] [2].

Split-ring resonator (SRR) and complementary split-ring resonator (CSRR) are the two popular fundamental structures of metamaterials which offer negative permeability and negative permittivity [1–3]. SRR comprises two concentric metallic rings with splits at opposite sides and is one of the essential elements for creating metamaterial property. This structure can be available in Broad-side Coupled (BC-SRR) or Edge-Coupled (EC)-SRR as shown in the Figures 1(a) and (b), respectively. The EC-SRR structure contains two concentric metallic split rings fabricated on the top of the printed circuit board as shown in Figure 1(a), while in BC-SRR, outer ring printed on top side and inner ring on the bottom side of the dielectric board as shown in Figure 1(b) [3].

The device conducts as an LC circuit driven by external electromotive force. The frequency of resonance is given by

$$\omega_0^2 = \frac{2}{LC} = \frac{2}{\pi r_0 C_{pul} L} \tag{1}$$

where C_{pul} is the capacitance per unit length, L the total inductance of the SRR, and r_0 the mean radius of the SRR. In the EC-SRR, the particle induces a strong magnetic dipole, a strong electric dipole and

Received 19 October 2017, Accepted 28 November 2017, Scheduled 25 January 2018

* Corresponding author: Nambiyappan Thamil Selvi (thamilchelviece@gmail.com).

[1] KR College of Engineering, Periyar Maniammai University, Thanjavur, India. [2] TRP Engineering College, India. [3] Periyar Maniammai University, Thanjavur, India. [4] National Institute of Technology, India.

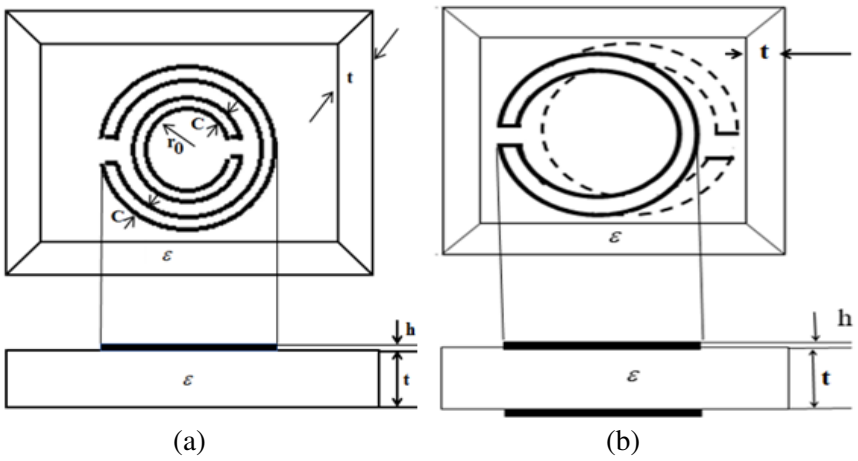

Figure 1. Schematic representation of fundamental (a) EC-SRR, (b) BC-SRR structure.

a strong polarizability near its resonance. The governing equations for the EC-SRR are as follows [3]:

$$m_z = \alpha_{zz}^{mm} B_z^{ext} - j\alpha_{yz}^{em} E_y^{ext} \tag{2}$$

$$P_y = \left(\alpha_{yy}^{ee} + \alpha_{yy}^{jee}\right) E_y^{ext} + j\alpha_{yz}^{em} B_z^{ext} \tag{3}$$

$$P_x = \alpha_{xx}^{ee} E_x^{ext} \tag{4}$$

where m and P are the magnetic and electric induced dipoles, and B^{ext} and E^{ext} are the external fields and α polarizabilities. From Equation (2), the EC-SRR has the possibility of cross polarization and bianisotrophy effects. Bianisotrophy effect is due to the existence of magnetoelectric coupling in the artificial constituents, which can be eliminated in the BC-SRR.

For BC-SRR, the governing equations are as follows:

$$m_z = \alpha_{zz}^{mm} B_z^{ext} \tag{5}$$

$$P_y = \alpha_{yy}^{ee} E_y^{ext} \tag{6}$$

$$P_x = \alpha_{xx}^{ee} E_x^{ext} \tag{7}$$

The utility of these structures in antenna design comprises electrically small multi-band antennas [4–15], which results in good impedance matching, gain and bandwidth enhancement [16–18]. Typical microstrips, flanges, strips and patches use semi analytical methods [23–29].

In this paper, the design, fabrication and characterization of a new compact coplanar waveguide (CPW) fed BC-SRR to achieve a dual-band antenna is explored. This structure consists of an outer ring of SRR on the top side and the inner ring of SRR on the bottom side. The proposed antenna is designed and optimized by using commercial finite-element package Ansoft HFSS version 13 and evaluated by microwave measurements.

2. ANTENNA DESIGN

The geometries of the proposed CPW-fed antenna's top and bottom views are shown in Figures 2(a) and (b). Figure 2(c) shows the perspective view of the proposed BC-SRR antenna. A BC-SRR resonant structure is introduced as the radiating element to produce a resonance. The proposed antenna is fabricated on a $31 \times 25 \times 1.6\,\text{mm}^3$ FR-4 epoxy substrate with a relative dielectric constant (ε_r) of 4.4 and loss tangent of 0.002. The antenna is fed by a CPW transmission line. Table 1 illustrates the dimensions of the proposed antenna. The prototype of the proposed antenna is fabricated and shown in Figure 3.

The parametric analysis comparison between simulated return loss characteristics of BC-SRR and EC-SRR of the proposed antenna is shown in Figure 4. It clearly shows that there is no significant resonance for the desired frequency band in EC-SRR configuration, but BC-SRR offers optimum dual

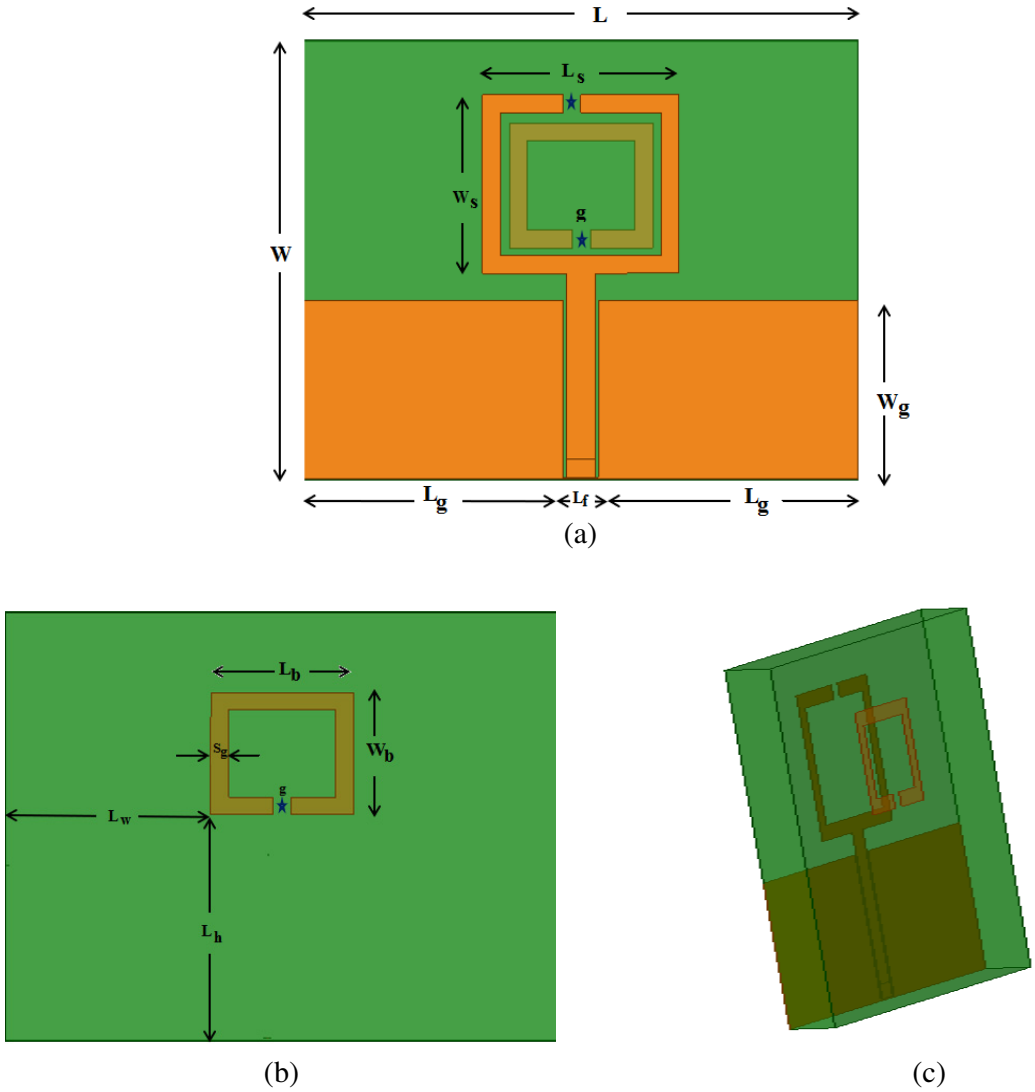

Figure 2. (a) Geometry of the proposed dual band BC-SRR inspired CPW fed antenna. (b) Geometry of bottom view of the proposed dual band BC-SRR inspired CPW fed antenna. (c) Perspective view of the proposed dual band BC-SRR inspired CPW-fed antenna.

Table 1. Dimensions of the proposed antenna.

Parameter		Parameter	Dimension (mm)
L	31	S_g & g	1
W	25	L_s	11
L_g	13.5	W_s	10
W_g	10	L_b	9
L_f	1.6	W_b	8
L_h	13	L_w	11.5

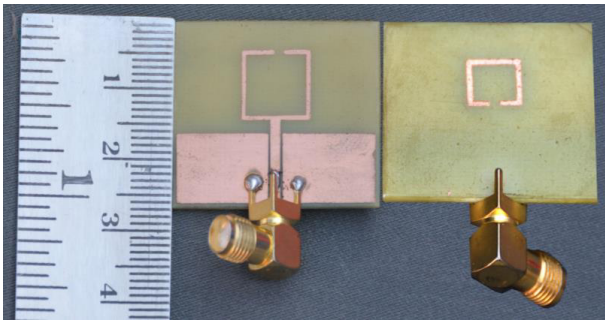

Figure 3. Photograph of fabricated BC-SRR inspired CPW-fed dual band antenna front and rear view.

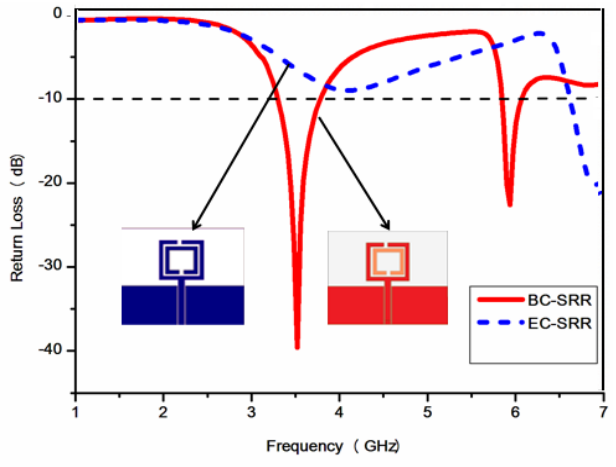

Figure 4. Simulated return loss of the basic BC-SRR and EC-SRR.

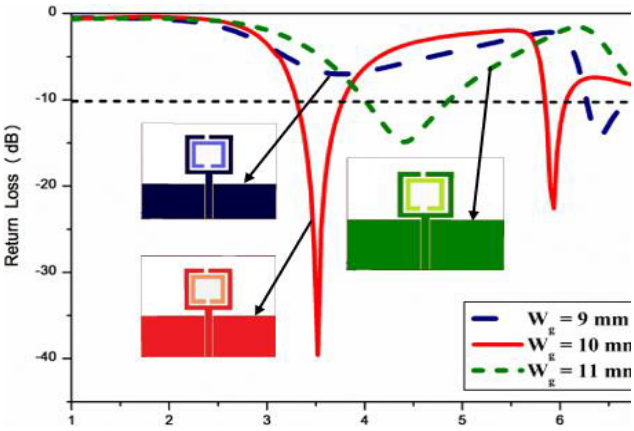

Figure 5. Simulated return loss for various values of ground plane width (W_g).

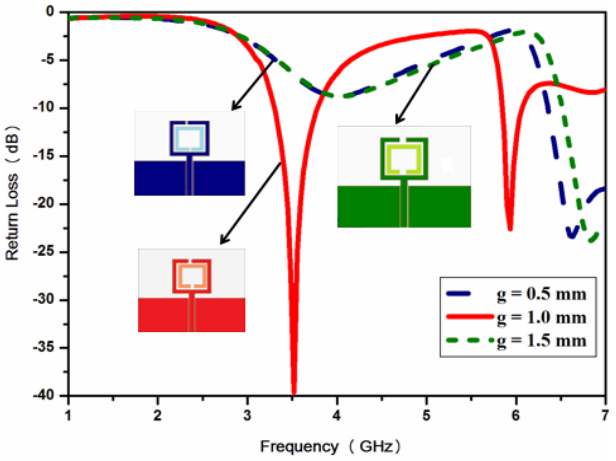

Figure 6. Simulated return loss for various split gap of proposed BC-SRR (g).

bands at 3.52 GHz and 5.92 GHz with the impedance bandwidth of 465 MHz (3.31–3.765 GHz) and 220 MHz (5.83–6.04 GHz), respectively.

The physical parameters of the ground plane width (W_g) and split gap (g) of the SRR are varied to obtain resonance at 3.52 GHz and 5.93 GHz. There is significant improvement by varying the height of the ground plane, and optimum frequency is observed for $W_g = 10$ mm, which is shown in Figure 5. The parametric analysis of split gap width is wide-ranging from 0.5 mm to 1.5 mm. The optimum resonance is obtained at 5.93 GHz with the split gap of 1 mm as shown in Figure 6.

The antenna's resonant modes are effectively understood by the simulated surface current distribution as shown in Figures 7(a) and (b), respectively. At 3.52 GHz, current distribution is primarily found in the feed line and periphery of the outer SRR's ring. The maximum current density is observed around the BC-SRR at the resonance frequency 5.93 GHz.

3. EXTRACTION OF NEGATIVE PERMEABLITY

The proposed BC-SRR is evaluated by the reflection coefficient (S_{11}) and transmission coefficient (S_{21}) to obtain negative permeability characteristics [19]. The parameter retrieval procedure for BC-SRR

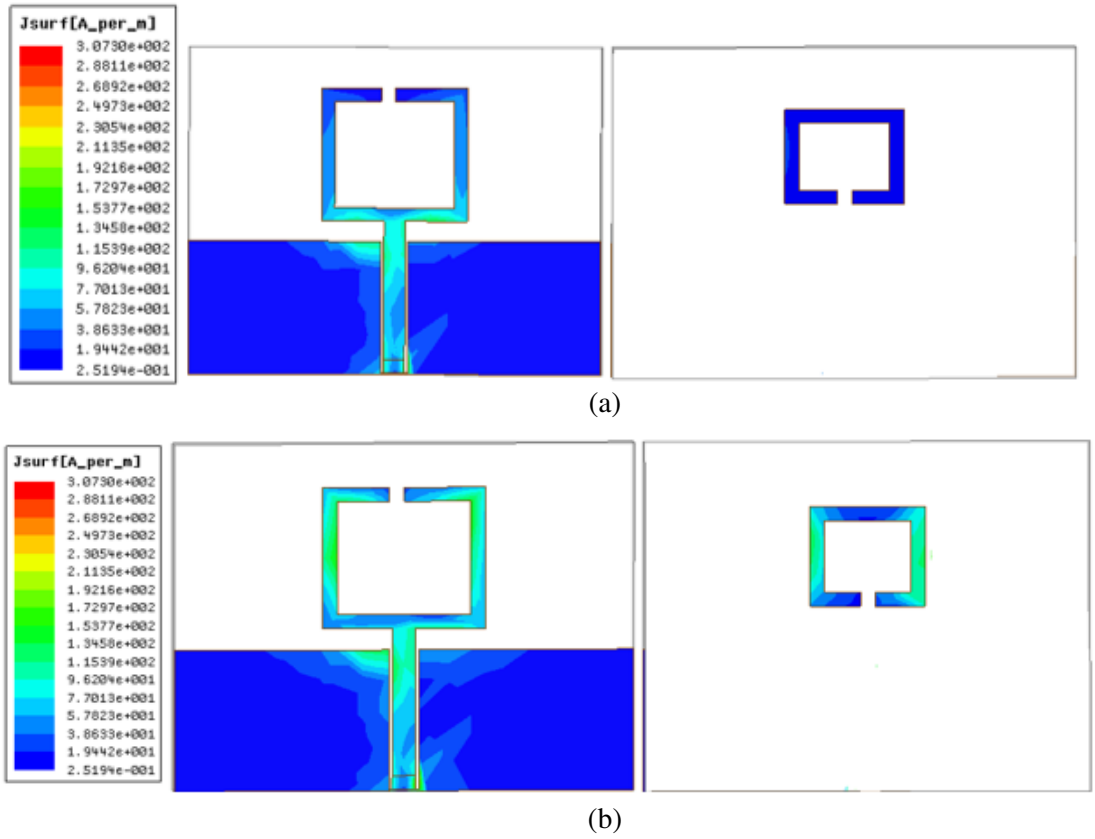

Figure 7. Simulated surface current distribution for the antenna at (a) 3.52 GHz, (b) 5.93 GHz.

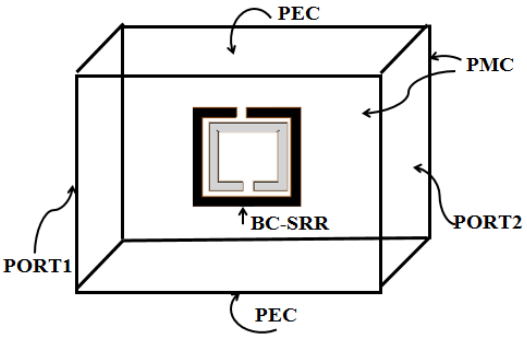

Figure 8. Wave guide setup to retrieve S_{11} and S_{21} parameters.

based on Nicholson-Ross-Weir (NRW) method is shown in Figure 8, which depicts the waveguide setup to extract the S_{11} and S_{21} parameters to obtain negative permeability characteristics.

The BC-SRR is excited by two lumped ports along the Y-axis, a Perfect Electric Conductor (PEC) along the X-axis and a Perfect Magnetic Conductor (PMC) along the Z-axis. MATLAB code is written for mathematical Equation (8) [20, 21]. Next, the permeability is calculated by,

$$\mu = n \times z \tag{8}$$

where

$$n = \frac{1}{kd}\cos^{-1}\left[\frac{1}{2S_{21}}\left(1 - S_{11}^2 + S_{21}^2\right)\right]$$

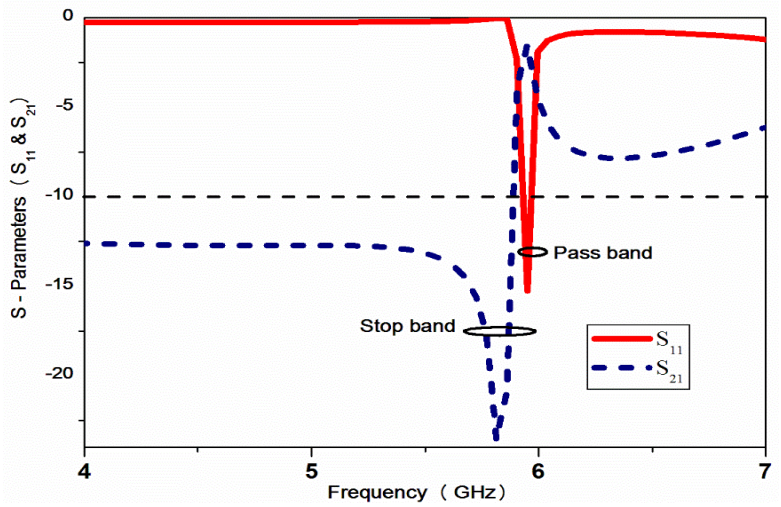

(a)

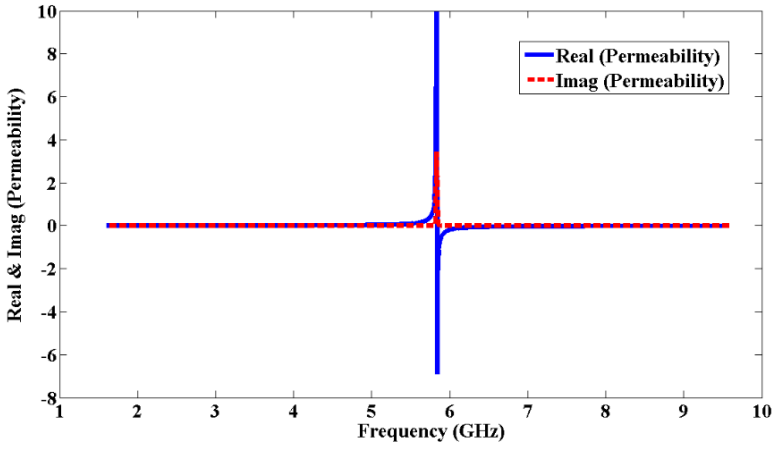

(b)

Figure 9. (a) Retrieval of S_{11} and S_{21} parameters. (b) Extracted negative permeability characteristics of the proposed BC-SRR.

$$z = \sqrt{\frac{(1+S_{11})^2 - S_{21}^2}{(1-S_{11})^2 - S_{21}^2}}$$

The S_{11} and S_{21} parameters are graphically shown in Figure 9(a). It shows the stopband characteristics of the BC-SRR at 5.8 GHz, where the reflection coefficient (S_{11}) is almost 0 dB, and the transmission coefficient (S_{21}) is at -35 dB. Similarly, the passband is inferred at 5.93 GHz. Thus, it is accountable for achieving new resonance around 5.93 GHz. The negative permeability (μ) of BC-SRR is obtained at 5.8 GHz as depicted in Figure 9(b).

Table 2 illustrates the comparison between the proposed antenna and the antennas listed in the reference in terms of shape, length and width along with the metamaterial property & quasi static analysis verification. It is observed that the proposed antenna has compact size.

4. QUASI STATIC ANALYSIS

Split gap is one of the core parameters of the SRR. If the split is removed, the BC-SRR will not produce any resonance frequency. Inductance of BC-SRR is due to the metallic strip and the capacitance due to

Table 2. Comparison of antenna performance.

Ref	Year	Antenna Size (mm × mm ×mm)	Patch Detail	Patch (mm × mm)	Feed	Frequency (GHz)	Metamaterial Property & Quasi static analysis
[4]	2013	31.7 × 27 ×1.6	Circular composite SRR and CSRR with trapeziform ground plane	7.5 × 3.1 ×4.5	CPW	2.6 & 3.6	Not Verified
[6]	2009	24 × 32 ×1.6	Rectangular SRR	16 × 13	Microstrip	2.41 & 5.36	Not Verified
[8]	2011	35 × 40 ×1.6	Triangular SRR	30 × 20	CPW	2.4, 3.5 & 5.5	Not Verified
[11]	2015	50 × 50 ×1.6	Defected Hexagon patch loaded with CSRR	12 × 8.8	Microstrip	2.62 & 3.23	Not Verified
Proposed	2017	31 × 25 ×1.6	BC-Coupled SRR	11 × 10	CPW	3.42 & 6.07	Verified

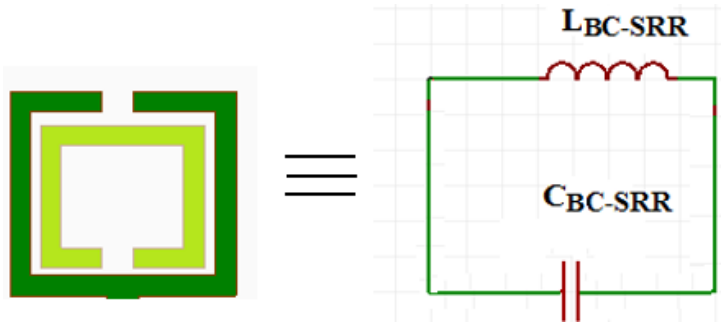

Figure 10. The equivalent circuit model of a proposed CPW-fed BC-SRR antenna.

the slot between the metallic strips. Application of Babinet principle leads to the Split Ring Resonator (SRR), and the CSRR is manipulated by the same expression. Analytical equivalent circuit model is shown in Figure 10. The steps to find the resonant frequency of the BC-SRR is as follows [22].

The expression of the inductance ($L_{\text{BC-SRR}}$) is given by,

$$L_{\text{BC-SRR}} = \frac{\mu_0}{2} l_{avg} \left[\ln\left(\frac{0.98}{\rho}\right) + 1.84\rho \right] \tag{9}$$

where $\rho = (N-1)(w+s)/[L_o - (N-1)(w+s)]$ is the filling ratio, μ_0 the vacuum permeability, L_o the side length of the external ring, w the width of the strips, and s the separation between two adjacent strips then,

$$l_{avg} = [L_o - (N-1)(w+s)]\,.$$

The expression for capacitance ($C_{\text{EC-SRR}}$) is given by,

$$C_{\text{BC-SRR}} = \frac{N-1}{2} [2L_o - (2N-1)(w+s)]\, C_0 \tag{10}$$

where N is the number of rings and C_0 the capacitance per unit length which is given as,

$$C_0 = \varepsilon_0 \frac{K\left(\sqrt{1-k^2}\right)}{K(k)}$$

where ε_0 is the vacuum permittivity, K the complex elliptic integral of first kind, and $k = s/(s + 2w)$.

Finally, the frequency of resonance is given by,

$$f_{\text{BC-SRR}} = \frac{1}{2\pi\sqrt{L_{\text{BC-SRR}}C_{\text{BC-SRR}}}} \tag{11}$$

The above mathematical equations are computed by the MATLAB code to estimate the inductance $L_{\text{EC-SRR}}$ and capacitance $C_{\text{BC-SRR}}$ values of BC-SRR. It is only suitable for the number of SRR rings greater than one ($N > 1$). For $N = 2$, $L_o = (L_s + W_s)/2 = 10.5\,\text{mm}$. The computed $L_{\text{BC-SRR}} = 8.4220e - 09$ (Henry) and $C_{\text{BC-SRR}} = 8.2622e - 14$ (Farad). Therefore, the resonance frequency of BC-SRR is $f_{\text{BC-SRR}} = 6.0333e{+}09$. The theoretically calculated resonance for the proposed BC-SRR antenna 6.0333 GHz is in agreement with the measured resonant frequency.

5. RESULTS AND DISCUSSION

The final design is fabricated as shown in Figure 3. The return loss characteristics are measured using the ENA series E5071C Vector Network Analyzer (VNA), shown in Figure 11. Figure 12 depicts

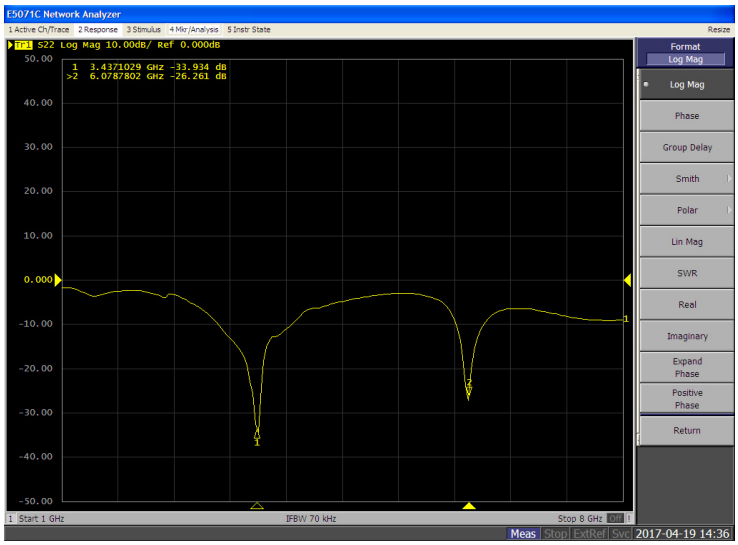

Figure 11. Measured return loss characteristics of proposed antenna in ENA series E5071C Vector Network Analyzer (VNA).

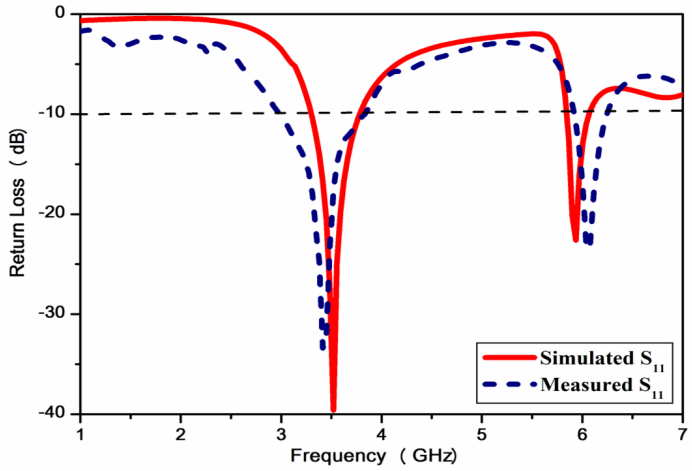

Figure 12. Simulated and measured return loss characteristics of the proposed antenna.

the comparison of simulated and measured return loss characteristics of the proposed antenna. The measured fundamental resonance of 3.42 GHz is observed with an impedance bandwidth of 840 MHz (3.00–3.84 GHz). The second resonance of 6.07 GHz occurs due to BC-SRR's with an impedance bandwidth of 310 MHz (5.94–6.25 GHz). Thus, it is applicable to WiMAX and WAVE applications.

The radiation pattern of the antenna is determined by keeping the antenna in an anechoic chamber. Figures 13(a) and (b) illustrate the simulated and measured co-polarization radiation patterns at 3.42 GHz and 6.07 GHz, respectively. It is obvious that the measured radiation pattern shows a dipole like radiation pattern in the E-plane and omnidirectional radiation pattern in the H-plane.

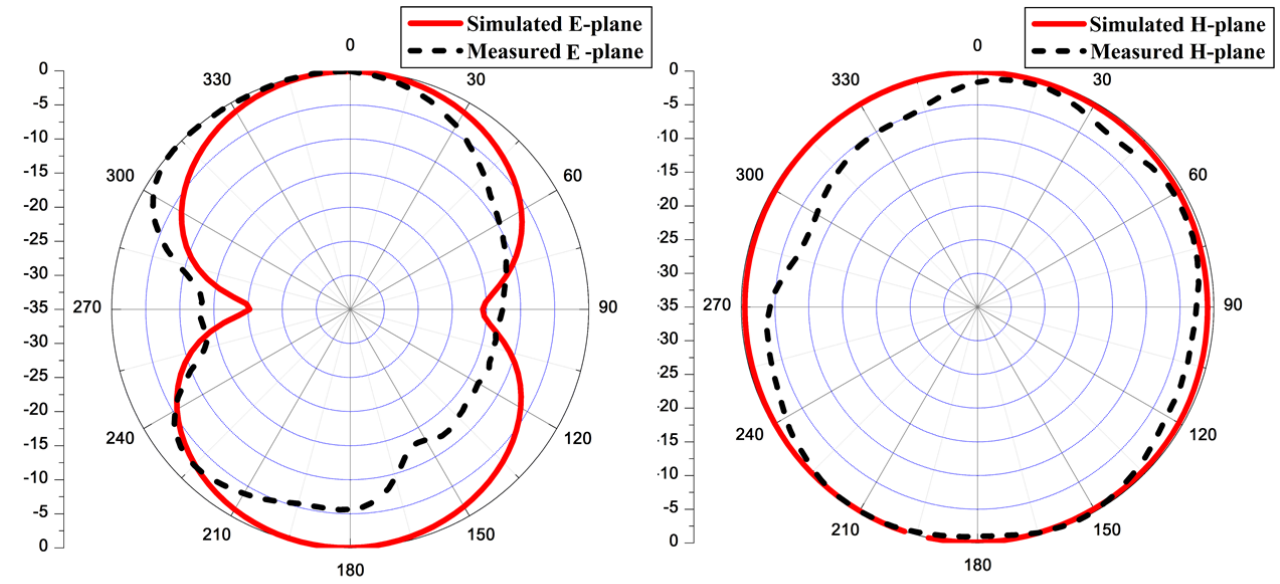

(a)

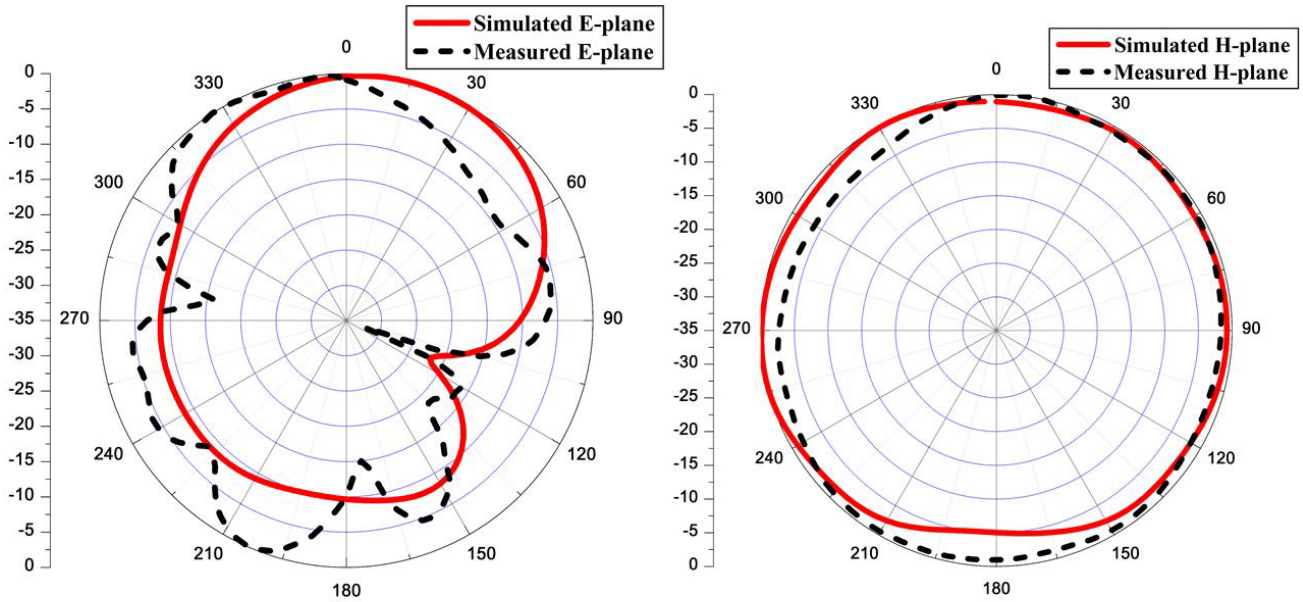

(b)

Figure 13. Simulated and measured E-plane and H-plane radiation patterns at (a) 3.42 GHz, (b) 6.07 GHz.

6. CONCLUSION

A novel broadside coupled split ring resonator inspired coplanar waveguide fed dual-band antenna with compact dimensions of $31 \times 25 \times 1.6\,\text{mm}^3$ for WiMAX and WAVE applications is presented. The parameters of split gap, ground width and BC-SRR model are parameterized to obtain optimum resonance. The negative permeability characteristics are also studied. The proposed antenna can be useful for WiMAX and WAVE applications. Hence, a BC-SRR loaded coplanar waveguide fed dual-band antenna is simulated, fabricated and agreed with experimental design. Good impedance matching and radiation characteristics are experiential for the operating bands. Moreover, electrically small size and low cost make the antenna ideally applicable to present and future wireless communication devices.

ACKNOWLEDGMENT

The authors would like to thank Dr. Vasudevan, Emeritus Professor, Department of Electronics, Cochin University of Science and Technology (CUSAT), Kerala, India for carrying out measurements.

REFERENCES

1. Veselago, V. G., "The electrodynamics of substances with simultaneously negative values of and μ," *Sov. Phys. Usp.*, Vol. 10, 509–514, 1968.
2. Caloz, C. and T. Itoh, "Electromagnetic metamaterials: Transmission line theory and microwave applications," *Wiley — IEEE Press*, New York, 2005.
3. Marqués, R., F. Martina, and M. Sorolla, "Metamaterials with negative parameters: Theory, design and microwave applications," *Wiley — Interscience*, 2007.
4. Si, L. M., W. Zhu, and H. J. Sun, "A compact, planar, and CPW-fed metamaterial-inspired dual-band antenna," *IEEE Antennas and Wireless Propagation Letters*, Vol. 12, 305–308, 2013, doi: 10.1109/LAWP.2013.2249037.
5. Erentok, A. and R. W. Ziolkowski, "Metamaterial-inspired Efficient electrically small antennas," *IEEE Transactions Antennas Propagation Letters*, Vol. 56, No. 3, 691–707, 2008, doi: 10.1109/TAP.2008.916949.
6. Basaran, S. C. and Y. E. Erdemli, "A dual band split ring monopole antenna for WLAN applications," *Microwave and Optical Technology Letters*, Vol. 51, 2685–2688, 2009, doi: 10.1002/mop.24708.
7. Liu, H.-W., C.-H. Ku, and C.-F. Yang, "Novel CPW-fed planar monopole antenna for WiMAX/WLAN applications," *IEEE Antennas and Wireless Propagation Letters*, Vol. 9, 240–243, 2010, doi: 10.1109/LAWP.2010.2044860.
8. Yang, K., H. Wang, Z. Lei, Y. Xie, and H. Lai, "CPW-fed slot antenna with triangular SRR terminated feed line for WLAN/WiMAX applications," *Electronics Letters*, Vol. 47, 685–686, 2011, doi: 10.1049/el.2011.1232.
9. Quan, X. L., R. L. Li, Y. H. Cui, and M. M. Tentzeris, "Analysis and design of a compact dual-band directional antenna," *IEEE Antennas and Wireless Propagation Letters*, Vol. 11, 547–550, 2012, doi: 10.1109/LAWP.2012.2199458.
10. Pandeeswari, R. and S. Raghavan, "A CPW-fed triple band OCSRR embedded monopole antenna with modified ground for WLAN and Wi-MAX applications," *Microwave and Optical Technology Letters*, Vol. 57, 2413–2418, 2015, doi: 10.1002/mop.29352.
11. Sharma, S. K. and R. K. Chaudhary, "Dual-band metamaterial-inspired antenna for mobile applications," *Microwave and Optical Technology Letters*, Vol. 57, 1444–1447, 2015, doi: 10.1002/mop.29113.
12. Rajeshkumar, V. and S. Raghavan, "A compact asymmetric monopole antenna with electrically coupled SRR for WiMAX/WLAN/UWB applications," *Microwave and Optical Technology Letters*, Vol. 57, 2194–2197, 2015, doi: 10.1002/mop.29298.

13. Imaculate Rosaline, S. and S. Raghavan, "A compact dual band antenna with an ENG SRR cover for SAR reduction," *Microwave and Optical Technology Letters*, Vol. 57, 741–747, 2015, doi:10.1002/mop.28941.
14. Rajeshkumar, V. and S. Raghavan, "Trapezoidal ring quad-band fractal antenna for WLAN/WiMAX applications," *Microwave and Optical Technology Letters*, Vol. 56, 2545–2548, 2014, doi: 10.1002/mop.28631.
15. Kaur, J. and R. Khanna, "Development of dual-band microstrip patch antenna for WLAN/MIMO/WiMAX/AMSAT/WAVE applications," *Microwave and Optical Technology Letters*, Vol. 56, 988–993, 2014, doi: 10.1002/mop.28206.
16. Pandeeswari, R. and S. Raghavan, "Broadband monopole antenna with split ring resonator loaded substrate for good impedance matching," *Microwave and Optical Technology Letters*, Vol. 56, 2388–2392, 2014, doi: 10.1002/mop.28602.
17. Pandeeswari, R. and S. Raghavan, "Microstrip antenna with complementary split ring resonator loaded ground plane for gain enhancement," *Microwave and Optical Technology Letters*, Vol. 57, 292–296, 2015, doi: 10.1002/mop.28835.
18. Pandeeswari, R. and S. Raghavan, "Meandered CPW-fed hexagonal split-ring resonator monopole antenna for 5.8 GHz RF-ID applications," *Microwave and Optical Technology Letters*, Vol. 57, 681–684, 2015, doi: 10.1002/mop.28920.
19. Smith, D. R., S. Schultz, P. Markos, and C. M. Soukoulis, "Determination of negative permittivity and permeability of metamaterials from reflection and transmission coefficients," *Phys. Review B*, Vol. 65, 195104–195109, 2002, doi: https://doi.org/10.1103/PhysRevB.65.195104.
20. Shelby, R. A., D. R. Smith, and S. Schultz, "Experimental verification of a negative index of refraction," *Science*, Vol. 292, No. 5514, 77–79, 2001, doi: 10.1126/science.1058847.
21. Chen, H., J. Zhang, Y. Bai, Y. Luo, L. Ran, Q. Jiang, and J. A. Kong, "Experimental retrieval of the effective parameters of metamaterials based on a waveguide method," *Optical Express*, Vol. 14, 12944–12949, 2006, https://doi.org/10.1364/OE.14.012944.
22. Bilotti, F., A. Toscano, L. Vegni, K. Aydin, K. B. Alice, and E. Ozbay, "Equivalent circuit models for the design of metamaterials based on artificial magnetic inclusions," *IEEE Transactionson Microwave Theory and Techniques*, Vol. 55, 2865–2872, 2007, doi: 10.1109/TMTT.2007.909611.
23. Valagiannopoulos, C. A., "On smoothening the singular field developed in the vicinity of metallic edges," *International Journal of Applied Electromagnetics and Mechanics*, Vol. 31, No. 2, 67–77, 2009, doi: 10.3233/JAE-2009-1048.
24. Fikioris, G. and C. A. Valagiannopoulos, "Input admittances arising from explicit solutions to integral equations for infinite-length dipole antennas," *Progress In Electromagnetics Research*, Vol. 55, 285–306, 2005.
25. Liu, W.-C., "Optimal design of dualband CPW-fed G-shaped monopole antenna for WLAN application," *Progress In Electromagnetics Research*, Vol. 74, 21–38, 2007.
26. Valagiannopoulos, C. A., "A novel methodology for estimating the permittivity of a specimen rod at low radio frequencies," *Journal of Electromagnetic Waves and Applications*, Vol. 24, Nos. 5–6, 631–640, 2010.
27. Valagiannopoulos, C. A., "Single-series solution to the radiation of loop antenna in the presence of a conducting sphere," *Progress In Electromagnetics Research*, Vol. 71, 277–294, 2007.
28. Liu, X. L., Y.-Z. Yin, P. A. Liu, J. H. Wang, and B. Xu, "A CPW-fed dual band-notched UWB antenna with a pair of bended dual-L-shape parasitic branches," *Progress In Electromagnetics Research*, Vol. 136, 623–634, 2013.
29. Valagiannopoulos, C. A., "High selectivity and controllability of a parallel-plate component with a filled rectangular ridge," *Progress In Electromagnetics Research*, Vol. 119, 497–511, 2011.